Light Scattering from Birefringent Sphere and Its Aggregation

Che-Min Chou and Po-Da Hong*

Department of Polymer Engineering, National Taiwan University of Science and Technology, Taipei, 10607, Taiwan

Received December 12, 2007; Revised Manuscript Received June 10, 2008

ABSTRACT: Recently, the new optics design offers the key to expand the depolarized small-angle light scattering (SALS) technique into complicated aggregation systems. We try to establish methodological basis especially for depolarized (H_v) scattering as applied to the recent advances in soft matter science. We give the scaled form factor $\tilde{P}_{H_v}(x)$ to study the universal feature of the H_v scattering from a birefringent sphere in nucleation and growth process. On the other hand, lacking the ability to describe the global-structure evolution, the structure factor scaling in aggregation and coarsening process of birefringent spheres are unsatisfactory for H_v scattering. However, the H_v and V_v (polarized) scattering complement each other well, for each captures a different aspect of the structural evolution of scatterers. The H_v scattering highlights the feature of the local-structure evolution; in contrast, the V_v scattering relates mainly to the feature of long-range fractal structure of aggregates. In order to understand the birefringence decline in a growing birefringent sphere, the two categories of birefringent sphere are considered, namely the crystallographic disorder (category 1) and the aggregation of crystallitic grains (category 2), and the PVDF microgel belongs to the category 2 and may be regarded as "soft colloids".

Introduction

Many early researchers believe that the physical gel is a homogeneous network, and the gel structure is well defined by a characteristic correlation length. This view can track back to the concept of the beginning from Flory[1] and de Gennes.[2] Thus, the majority of research in the physical gels has focused on the "microscopic" junction structure and the "macroscopic" viscoelastic properties. Guenet[3] and te Nijenhuis[4] have provided extensive discussions on the subjects. However, the traditional viewpoint ("equilibrium") and classification ("junction basis") frequently do not give a realistic description of how the diverse and hierarchical morphologies of physical gels are formed. Most researchers have up to now employed "morphological criteria" to—imaginatively—reconstruct the gelation process.[5,6]

In our previous studies,[7,8] we have found that the isolated droplets formed by nucleation and growth may aggregate together to form a gel network if the volume fraction of droplets is above a critical threshold and the droplets have a feature of the hard-sphere systems. Now we call it "nucleation gel". Three concepts emerge for the description of nucleation gel. First, unlike the traditional viewpoint,[1−6] the definition of nucleation is not on the localized junction "point" but really involves a mesoscopic length scale over; thus, the focus of the "gelation" shifts from an emphasis on the percolation phenomena[9,10] to attention to the aggregation behavior. Second, even though the large-scale heterogeneous gels are widely believed to result from spinodal decomposition ("spinodal gel"),[11−15] their formation might be of a rather different origin. Third, the nature of nucleation gel is purely nonequilibrium phenomena, and the concept itself blurs the boundary between the gel ("elastic" and three-dimensional network structure) and the jammed solid ("fragile" and nonequilibrium solid state).[16,17] While most research on gel structure has been descriptive, we try to explore the origin of the diverse morphologies. The nucleation gel gives us new opportunities to dealing in a more general manner with the physical gelation.

In general, the gelation process cannot be reconstructed from any one of the "static" micro- or thermal-analytical technique. At this point, the time-resolved SALS (small-angle light scattering) technique may play a critical role in obtaining "real-time" information on aspects of a complex event in physical gelation.[7,8] However, using depolarized SALS to trace and reconstruct the dynamic evolution of a mesostructure such as the nucleation gel is still a developing "new" technique, and many methodological problems need to be overcome. Before moving on to the main task, we should briefly review an early development and several controversial problems in SALS.

Stein and co-workers were the pioneers in the SALS technique and provided comprehensive treatments of light scattering from polymeric spherulites.[18−22] They concluded that the H_v scattering arises entirely from the optical anisotropy of the scatterer while the V_v scattering is attributed to both the optical anisotropy and the density fluctuation in the system.[18] However, the validity and the generality of their view were later challenged by the experimental result of the H_v scattering from an amorphous (optical isotropy) sphere.[23,24] Meeten and co-workers attributed the problem to the coupling between the "scattering" properties of the scatterer and the "optical transmission" properties of the analyzer in the original Stein−Rhodes theory (SR theory),[25,26] and the coupling relationship inherently confines the SR theory to the case of polymeric spherulites. Hence, the first step in expanding the depolarized SALS technique into complicated aggregation systems is to decouple such a confused relationship. On the basis of the scattering matrix theory,[27] Meeten and co-workers[23−26] have given a more general treatment, and our studies would build under their framework.

So far, however, no specific approach has touched on how to extract all the structural information contained in H_v scattering pattern. Here, we would address some important questions to establish the methodological basis, especially for depolarized SALS as applied to the complicated aggregation systems. To that end, the following questions need to be considered in advance: What is the implication of the birefringence decline on studying the structure of scatterers? Is the H_v form factor of growing spherulite or birefringent sphere possible to have a scaling relationship? Does the common behavior of structure factor scaling still hold in aggregation and coarsening process of birefringent spheres? From a practical point of view, answering these questions lays the groundwork for understanding of how to extract the common and universal features of the

* Corresponding author: Fax +886-2-27376544; e-mail poda@mail.ntust.edu.tw.

10.1021/ma702765u CCC: $40.75
Published on Web 07/26/2008

dynamic evolution of a mesostructure from very different physical phenomena (i.e., growth and form of spherulites, physical gelation, and colloidal aggregation). To our knowledge, these issues are under-researched and under-discussed, not to mention a paucity of literature. We believe that findings will have broad implications in the recent advance in soft matter science.[28–30]

Experimental Section

Materials. The crystalline polymer used in this study was poly(vinylidene fluoride) (PVDF) powder ($M_w = 2.75 \times 10^5$ and $M_w/M_n = 2.57$, Aldrich Chemical Co.). The solvent was a mixture of tetra(ethylene glycol) dimethyl ether (TG) and $LiCF_3SO_3$ salt. The salt was added to give an O:Li ratio (oxygen atoms in TG: lithium atoms in the salt) of 12:1. The polymer gel electrolytes were prepared by quenching homogeneous PVDF solution from 433 K to the gelation temperature.

Time-Resolved SALS Apparatus. The optical arrangement of the time-resolved SALS apparatus has been described previously.[8] A 5 mW polarized He−Ne laser was used as the incident source, and the polarization direction of the beam was adjusted by a half-wave plate. The beam was then spatially filtered, expended, and shined onto the sample. The sample cell was placed on THMS 600 heating and freezing stage (Linkam Scientific Co.), and the scattered light intensity was directly imaged through a Fourier lens and an analyzer onto the CCD camera (Apogee Instruments Inc., Alta U2000 CCD camera). The digitized images were transferred the real-time processing to a personal computer. In the present study the reliable data are about $\theta = 0.8°-22.5°$, corresponding to $q = 0.2-5.56\ \mu m^{-1}$ [$q = (4\pi m_1/\lambda)\sin(\theta/2)$, where q is the scattering vector, λ is the wavelength of incident light, and m_1 is the refractive index of an isotropic medium].

Results and Discussion

From the Meeten−Navard theory (MN theory), the light scattered by a birefringent sphere is described by[26]

$$I_{H_v} = \frac{I_0}{k^2 r_0^2}|S_2 - S_1|^2 \sin^2 2\varphi \quad (1)$$

and

$$I_{V_v} = \frac{I_0}{k^2 r_0^2}|S_1 \sin^2\varphi + S_2 \cos^2\varphi|^2 \quad (2)$$

where I_0 is the incident light intensity, k is the wavenumber $2\pi/\lambda$, r_0 is the distance between detector and scatterer, and φ is the azimuthal angle. The expressions for S_1 and S_2 in the Rayleigh−Gans−Debye light scattering approximation are[26]

$$S_1 = \frac{2ik^3a^3}{3x^3}\{3(\mu-1)(\sin x - x\cos x) + \Delta\mu[x\cos x - 4\sin x + 3\,\mathrm{Si}(x)]\} \quad (3)$$

and

$$S_2 = \frac{2ik^3a^3}{3x^3}\{3(\mu-1)(\sin x - x\cos x)\cos\theta - \Delta\mu[1+\cos^2(\theta/2)][x\cos x - 4\sin x\,\mathrm{Si}(x)]\} \quad (4)$$

where a is the spherical radius, x is defined by $x = qa$, μ is the relative mean refractive index of the sphere, $\Delta\mu$ is the birefringence index, and $\mathrm{Si}(x)$ is the sin integral defined by

$$\mathrm{Si}(x) = \int_0^x \frac{\sin u}{u}\,\mathrm{d}u \quad (5)$$

If the birefringent sphere is surrounded by an isotropic medium of refractive index m_1, then μ is defined by $\mu = (m_r + 2m_t)/3m_1$ and $\Delta\mu$ is defined by $\Delta\mu = (m_r - m_t)/m_1$, where m_r and m_t are the radial and the tangential refractive indices of the sphere,

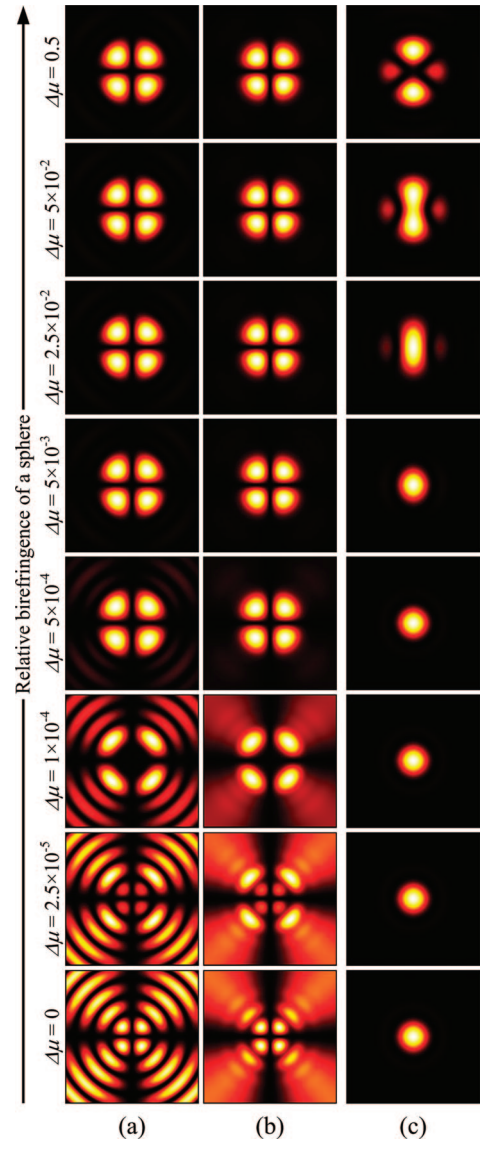

Figure 1. Calculated scattering patterns for a birefringent sphere as a function of the relative birefringence $\Delta\mu$. The sphere radius is 2 μm, $\mu = 0.991$, $m_1 = 1.433$, and $\theta = 0°-25°$. (a) H_v scattering; (b) H_v scattering with a size distribution for $\beta = 0.25$; (c) V_v scattering.

respectively. Generally, the appropriate size distribution could aid us to compare the discrepancy between the experimental and the theoretical scattering patterns. Assuming no correlation between the spheres, the scattered intensity can be regarded as the sum of the intensities scattered by individual spheres; thus[31]

$$I = \int_0^\infty N(a)\, I(a)\, \mathrm{d}a \quad (6)$$

where $N(a)$ is a size distribution function of the sphere. As the simplest example we assumed a Gaussian distribution function

$$N(a) = \exp\left[-\frac{1}{2}\left(\frac{a-a_0}{\beta}\right)^2\right] \quad (7)$$

where a_0 is average radius of the spheres in the distribution and β is the half-width of the distribution.

In Figure 1, we show how the birefringence of the sphere affects the scattering patterns. A series of the H_v and the V_v patterns calculated from eqs 1–5 are shown in Figure 1a,c by taking $a_0 = 2\ \mu$m, $\mu = 0.991$, and $m_1 = 1.433$. For the sake of qualitative discussion, the scattering intensity distributions of the calculated patterns were shown by arbitrary units. The top patterns ($\Delta\mu = 0.5$) are for a polymeric spherulite and are in

broad agreement with many experimental observations.[18] The bottom patterns ($\Delta\mu = 0$) corresponds to the light scattering by an amorphous sphere, which has been established experimentally by Desbordes et al.[24] Figure 1b shows the size distribution effect on the H_v patterns for $\beta = 0.25$. We observe a significant broadening and smoothing in the scattering patterns; especially at large scattering angles, the higher-order maxima are eliminated by averaging intensities over a distribution of sphere size. As seen in the Figure 1, when the birefringence of the sphere is decreased, the changes in the shape of the scattering patterns are observed.

The question now arises: what is the implication of the birefringence decline on studying the structure of scatterers? Before turning to this issue, we would like to recall Stein and co-workers' angle. The SR theory stressed the attributive difference between H_v and V_v scattering; thus, one can separate the contributions of the density and the anisotropy (orientation) fluctuations from H_v and V_v scattering intensities.[19,21] Although in the case of polymeric spherulites, however, the findings differ quantitatively from theory, especially a significant excess intensity at large scattering angles. To solve this problem, Stein and co-workers developed a lattice theory and ascribed the excess scattering intensity to the internal disordered of the spherulite.[22] Since the limitation of original theory, the Stein's lattice theory holds if the orientational disorder in spherulite is rather small. Nevertheless, in principle, the Stein's lattice theory provides access to a structural analysis of spherulite. Given that the spherulitic birefringence decreases as the disorder increases, we can explain the structural implication of the birefringence decline. However, in contrast with MN theory, Stein's lattice theory is unavoidably complex, difficult to apply, and not readily extensible to aggregate systems. From our position, these two theories complement each other; MN theory gives a general framework to describe the birefringence decline, while Stein's lattice theory further enables the decline to have structural implication. As shown in Figure 1b, when $\Delta\mu$ is decreased, a slight increase in the excess intensity at large scattering angles is observed. As $\Delta\mu = 0$ is approached, a well-defined double structure is gradually formed.

Generally, the birefringent sphere depends on two ways: one is the crystallinity of the sphere, and the other is the orientation direction of crystalline lamellae within the sphere. For a melt-crystallized polymer, spherulites are the ubiquitous morphology which the crystalline lamellae grow radially from the nucleation site. In the case, the optic axes of crystalline lamellae have a high orientation in the growth direction. The top three rows in Figure 1 show the typical scattering patterns for the polymeric spherulites. The variations in top three rows are referred to the polycrystalline nature and to containing an amorphous phase between the crystalline lamellae. It is interesting to note that the shape of the V_v scattering patterns is more sensitive to $\Delta\mu$.

The middle two rows in Figure 1 show the characteristic of the birefringent sphere, which is first observed in the PVDF gels. One can see the typical four-leaf-clover H_v patterns and the circularly symmetrical V_v patterns. So far, $\Delta\mu$ is linked with the internal disordered of the sphere and, more specifically, the orientation direction of the optic axes of crystalline lamellae within the sphere. This drives us to the question what the structural model of the birefringent sphere is. There are two main categories of birefringent sphere. Category 1 is the crystallographic disorder. On the basis of the phase filed theory, Gránásy et al.[32] presented a model that incorporates the growth front nucleation and the diffusional instabilities to describe the morphological variability of polycrystalline spherulites. In the case of a needle-shape single crystal, the growth front nucleation and the randomization of the local crystallographic orientation lead to form a "loose fungous spherulite" and depress the

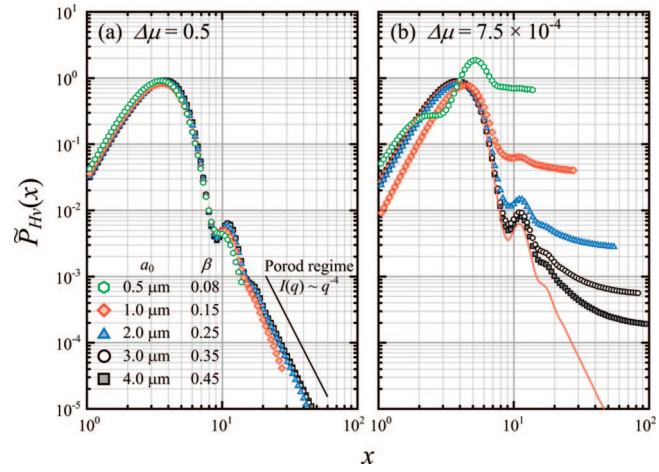

Figure 2. Scaling behavior of the calculated form factor for (a) strongly and (b) weakly birefringent sphere. The relative mean refractive index of the sphere is 0.991 and $m_1 = 1.433$.

birefringence of the sphere. Category 2 is the aggregation of crystallitic grains. Essentially, the category 2 is an intuitive hypothesis and should be demonstrated through the empirical investigation. The two categories may be of importance in explaining the structural formation of the PVDF microgels, which is the key feature of the nucleation gel.

A wide variety of systems and processes present the same features in the late stage of growth, aggregation, or coarsening; thus, the time evolution of the scattering function can be scaled with a single time-dependent length parameter. It would seem advisable to identify the structure of the growing PVDF microgels through the scaling analysis of scattering form factor. Surprisingly, although light scattering from polymeric spherulites has been an object of study for long time, whether the scattering function can be scaled has never been examined. In addition to explore the structure of the microgels, overcoming the scaling problem can be of enormous value to the methodology of the depolarized SALS.

The concept of dynamical scaling hypothesis, introduced by Binder as a way of approaching the time evolution of the scattering function,[33,34] now has many fields of application such as spinodal decomposition, fractal aggregation, colloidal gelation, and colloidal crystallization. In the two-phase system, the scattering function is given by[35]

$$I(q) = V\langle\eta^2\rangle \int \gamma(\mathbf{r}) e^{-iq\mathbf{r}}\, d\mathbf{r} \tag{8}$$

where V is scattering volume, $\langle\eta^2\rangle$ is the mean-square density fluctuation, and $\gamma(\mathbf{r})$ is the correlation function. Generally, for time-evolution structure, the scattering function is given in terms of the universal scaling function $\tilde{S}(x)$[36]

$$I(q,t;T) \sim \langle\eta^2(t;T)\rangle\, q_m^{-d}(t;T)\tilde{S}(x) \tag{9}$$

where $q_m(t;T)$ is the characteristic wavenumber of fluctuations at time t and temperature T, d is the growth dimension, and x is defined by $x = q/q_m(t;T)$. The scaled structure factor $F(x,t)$ is defined by[36]

$$F(x,t;T) = q_m^d(t;T)\, I(x,t;T) = \langle\eta^2(t;T)\rangle\, \tilde{S}(x) \tag{10}$$

For the case of the late-stage spinodal decomposition, the $\langle\eta^2(t;T)\rangle$ reaches the equilibrium value, and then the $F(x,t;T)$ becomes universal with time $F(x,t;T) \sim \tilde{S}(x)$. The major purpose of the studying scaled structure factor is to determine the universal structure features $\tilde{S}(x)$ in the growth and evolution of aggregation systems. The same is true of scaled form factor. For a nucleation and growth system, the volume fraction of

growing new phase is the function of time. In order to obtain a universal feature, the time evolution of the scaled form factor should be reduced with the invariant Q. For H_v scattering, the scaled form factor $\tilde{P}_{H_v}(x)$ is defined by

$$\tilde{P}_{H_v}(x) = I^{45^\circ}_{H_v}(x, t) q_m^d(t)/Q \tag{11}$$

where d is the growth dimension and q_m is the scattering vector at peak position. The invariant Q is defined by

$$Q = \int_0^\infty I^{45^\circ}_{H_v}(q) q^2 \, dq \tag{12}$$

On the basis of the MN theory, the invariant in the H_v scattering is ascribed to both mean-square optical anisotropy $\langle \delta^2 \rangle$ and the mean-square density fluctuation $\langle \eta^2 \rangle$. A problem now arises: due to the excess scattering intensity of which arises from $\langle \eta^2 \rangle$, $I^{45^\circ}_{H_v}(q) q^2$ shows a divergent behavior in high-q regime, and the value of Q does not converge to a constant. To avoid this problem, we may expediently neglect the isotropic term in eqs 3 and 4 to calculate the equivalent invariant Q_{an} and[21]

$$Q_{an} \propto \langle \delta^2 \rangle = \phi_s \Delta\mu^2 \tag{13}$$

where ϕ_s is the volume fraction of the birefringent sphere. Thus, we can clarify the relative contribution of the volume fraction of the growing new phase on the scaled form factor.

To test the validity of the scaled form factor, we show the calculated form factor for strongly and weakly birefringent sphere in Figure 2. Figure 2a shows a universal behavior for all x range, confirming the validity of $\tilde{P}_{H_v}(x)$ given by eq 11. In addition, at $x > 10$, $\tilde{P}_{H_v}(x)$ shows the characteristic of Porod's law (q^{-4} behavior).[35] It is clear that $\tilde{P}_{H_v}(x)$ can be ubiquitously observed in growth of polymeric spherulites from the melt. On the other hand, for the weakly birefringent sphere (Figure 2b), $\tilde{P}_{H_v}(x)$ is not universal with a_0 due seemingly to the contribution of the excess scattering intensity in high-q regime; moreover, $\tilde{P}_{H_v}(x)$ has diverse features at all x the range. However, we assumed a homogeneous sphere and used constant $\Delta\mu$, μ, and m_1 to calculate the form factor only as convenient descriptions of the common behavior (the ideal two-phase system or the growth of spherulite in the melt). The result in Figure 2b seems to contradict the general supposition. In the absence of experimental evidence, no definite conclusion can be drawn. Actually, in contrast with the polymeric spherulites, the structure of the birefringent sphere may have a morphological diversity and may concern a complex formation process, e.g., the PVDF microgels.

To test the generality of the scaled form factor, we analyze the time evolution of the $\tilde{P}_{H_v}(x)$ for the PVDF microgels in nucleation and growth stage, as shown in Figure 3. We also fit the scattering profile for $t = 1805$ s to obtain the optimum values of a_0, μ, $\Delta\mu$, m_1, and β; the fitting result is shown by the sold line in Figure 3. While not in perfect agreement, the result captures the overall characteristics of the PVDF microgels. As we have seen, the existence of a single master curve certifies that $\tilde{P}_{H_v}(x)$ holds in the growth of the birefringent sphere in the solution. This behavior is reminiscent of spinodal decomposition in binary mixtures; however, to our knowledge, theoretical predictions or experimental evidence for $\tilde{P}_{H_v}(x)$ did not exist. The experiment has highlighted several interesting possibilities: because the concentration of the solute in surroundings decreases as the nuclei grows, the values of $\Delta\mu$, μ, and m_1 are the functions of the nuclei size; thus, the structure of the PVDF microgels may have a self-similar characteristic. To understand these behaviors, we would begin our discussion by reviewing two recent experimental results. In studying PVDF aggregate in the dilute concentration state, Park et al.[37] found that the PVDF chains aggregate to form a core−shell structure with unexpectedly high R_H/R_G ratio ($R_H/R_G \sim 1.45$ and $R_H \sim 300$ nm, where

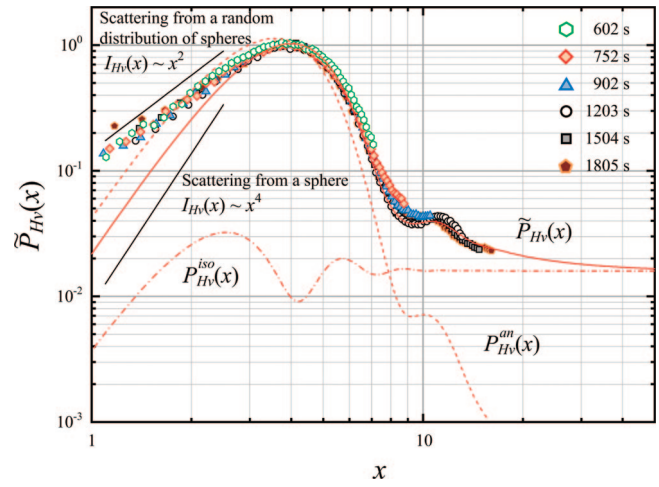

Figure 3. Scaled form factor in the nucleation and growth stage for PVDF/TG-$LiCF_3SO_3$ solution ($\phi = 0.04$) at 293 K. The solid line is the best theoretical fit for the experimental scattering profile ($t = 1805$ s) with $a_0 = 2.9945$ μm, $\mu = 0.994$, $\Delta\mu = 9.842 \times 10^{-5}$, $m_1 = 1.4286$, and $\beta = 0.472$. The dashed line and the dash-dotted line are the contributions of the anisotropic and isotropic terms, respectively.

$R_H/R_G = 1.291$ for hard sphere) even in good solvents. On the other hand, in studying protein crystallization from solutions, Vekilov et al.[38,39] have indicated that the structure fluctuation (to form an order structure) follows and is superimposed upon the density fluctuation (to form a dense liquid phase) during the nucleation process. From Vekilov's angle, the dense liquid core formed by PVDF chains aggregate may transform into an ordered crystalline nucleus through the structure fluctuation. This means the existence of crystalline microcolloids dispersed in the solution. To put the argument more concretely, we may conclude the PVDF microgel as a spherical cluster formed by the aggregation of the crystalline microcolloids belongs to the category 2 birefringent sphere. However, it is not to say that the structure and the structural formation of the PVDF microgels have the characteristic of fractal aggregation kinetics. In fact, this problem may be excluded by considering the $q_m{}^3$ behavior in $\tilde{P}_{H_v}(x)$, which depends on the dimension of growth and corresponds to the three-dimensional cluster growth, and the feature of $\tilde{P}_{H_v}(x)$ at $4 < x < 10$, which is relevant to the global structure of scatterer and is consistent with the calculated form factor. Although lacking definite information, we assume that the aggregation of crystalline microcolloids is essentially corresponding to the classical picture of nucleation phenomenon.

At $x < 4$, the experimental $\tilde{P}_{H_v}(x)$ shows a significant departure from the calculated one. If the asymptotic behavior of x^4 reflects the characteristic of a sphere, the x^2 behavior seems to imply the feature of the Ornstein−Zernike form [$S_{OZ}(q) \sim 1/(1 + q^2\xi^2)$, where ξ is the correlation length].[35] However, the Ornstein−Zernike equation is often used to analyze the concentration fluctuation in single-phase region. This seems to contradict the present system. Moritani et al. have given a general treatment of scattering from a random distribution of spherical domain structure.[40] Discussing the long-range correlation of the dispersed spheres is irrelevant to the main subject of this paper. This point may well be left to our future work.

Figure 4 shows the phase-contrast microscopy of a common representative of PVDF gels. It is clear that the PVDF gel exhibits spheroidal morphology and the spheres are connected with each other to form a three-dimensional network structure. Such morphology has been observed in the majority of PVDF gels or membranes.[41−43] From the phenomenological point of view, in contrast with the traditional viewpoint,[1−6] the nucleation gel usually accompanies a complicated aging effect (the

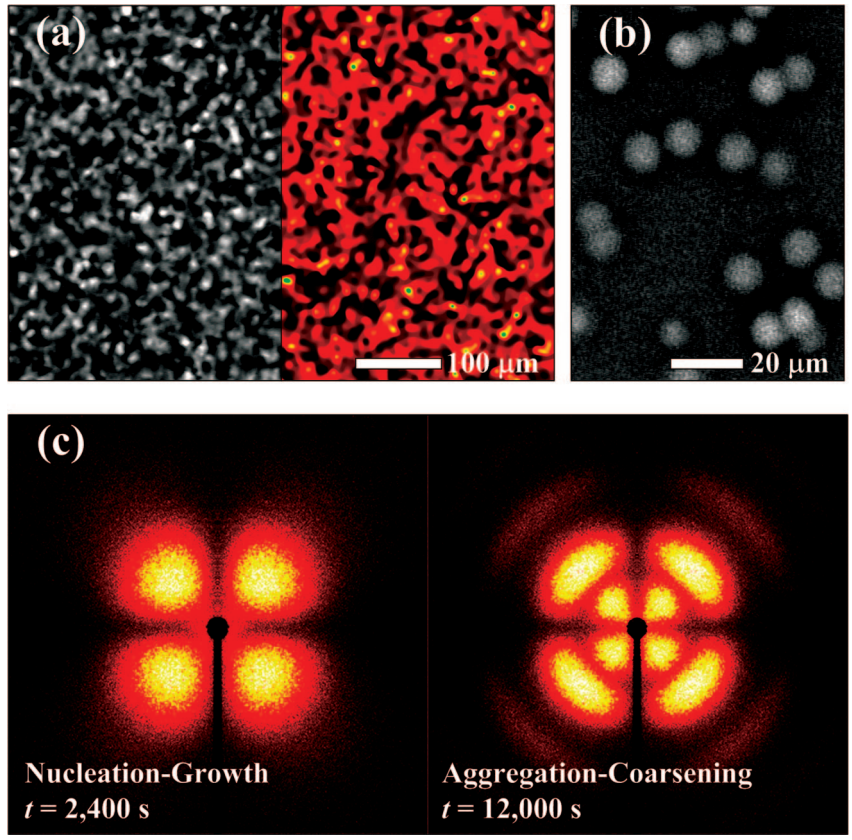

Figure 4. Phase-contract microscopy of PVDF gels, prepared by $\phi = 0.023$ solutions at 303 K. (a) Left: the raw image of growth in the quartz crucible with 1.8 mm depth; right: the analysis image using a ring around every pixel to calculate the median. (b) Put the sample in two coverslips, gap spacing <30 μm. (c) The representative of H_v scattering patterns for $\phi = 0.04$ at 293 K in nucleation and growth stage and coarsening stage, respectively.

restructuring of gel).[7,44] As shown in Figure 4a, the gel is formed by a random packing of the PVDF microgels. Thus, as the nuclei grow, the dynamics of the microgels is suddenly arrested by the spatial constraint and the attractive interactions between the particles, which ultimately form the space-filling disordered solid. It seems reasonable to assume that the origin of nucleation gel may be related to the jamming transition.[16,29] However, the jamming is characterized by "dynamic arrest";[45] the present results, as probed by "static" light scattering, lack the ability to support this assumption. Whether the above argument holds truth is an open question, the concept of nucleation gel may give rise to a new insight and more innovative possibilities on the physical gelation. Future research is obviously required; we intend to continue pursuing this subject in a series of experimental studies.

The nucleation gel also exhibits a local ripening in late-stage coarsening process. Figure 4b shows the feature of interpenetrated spheres. Because of the broad particle size distribution and the hard-sphere contract in system (i.e., high specific surface), the system tries to minimize its interfacial energy by Ostwald ripening.[46,47] The ripening process may take place via the crystalline microcolloids dissolution from small microgels and reprecipitation on the surface of backbone of the gel network or the necks between the microgels.[7] Besides reducing the interfacial free energy, the ripening process may yield positive effects on network strength. These findings also mean that the PVDF microgels may be regarded as "soft colloids". All of these are attributable to that the PVDF microgel is a spherical aggregation of the crystalline microcolloids.

Figure 4c shows the representative of H_v scattering patterns in nucleation and growth stage and coarsening stage. We have proposed some phenomenological functions to describe the complicated patterns of the nucleation gel. In our model, the scattered intensity $I(q)$ from birefringent sphere and its aggregation can be written as[7]

$$I(q) \sim P(q)\, S(q)\, f(q) \tag{14}$$

where $P(q)$ is the form factor (i.e., the scattering function for a birefringent sphere along and expressed by eqs 1 and 2), $S(q)$ is the structure factor (i.e., the spatial arrangement of the spheres within an aggregate and usually displaying a scaling behavior), and $f(q)$ is the interference function of two interpenetrated spheres (i.e., related to the evolution of local structure during the late-stage coarsening process). Here the structure factor for the fractal aggregate is given by[48]

$$S(q) = 1 + \frac{D_f \Gamma(D_f - 1)}{(qa_0)^{D_f}(1 + 1/q^2\xi^2)^{(D_f-1)/2}} \sin[D_f - 1) \tan^{-1}(q\xi)] \tag{15}$$

where D_f is the fractal dimension, ξ is the characteristic correlation length of the aggregate, and $\Gamma(x)$ is the gamma function. The interference function of two interpenetrated spheres can be written as[7,49]

$$f(q) = \frac{\frac{1}{2} + J_0(2ka_rF \sin\theta)}{a_r^2\left(2\pi - 3 \arccos F + 2F\sqrt{1 - F^2}\right)} \tag{16}$$

where J_0 is the zero-order Bessel function,a_r is the time-dependent coarsening size, and F is the overlapping parameter defined by $F = a_0/a_r$. For two spheres in hard-sphere contact, $F = 1$. If the coarsening of two contact spheres, $F < 1$. The $f(q)$ is important in laying the groundwork for studying how

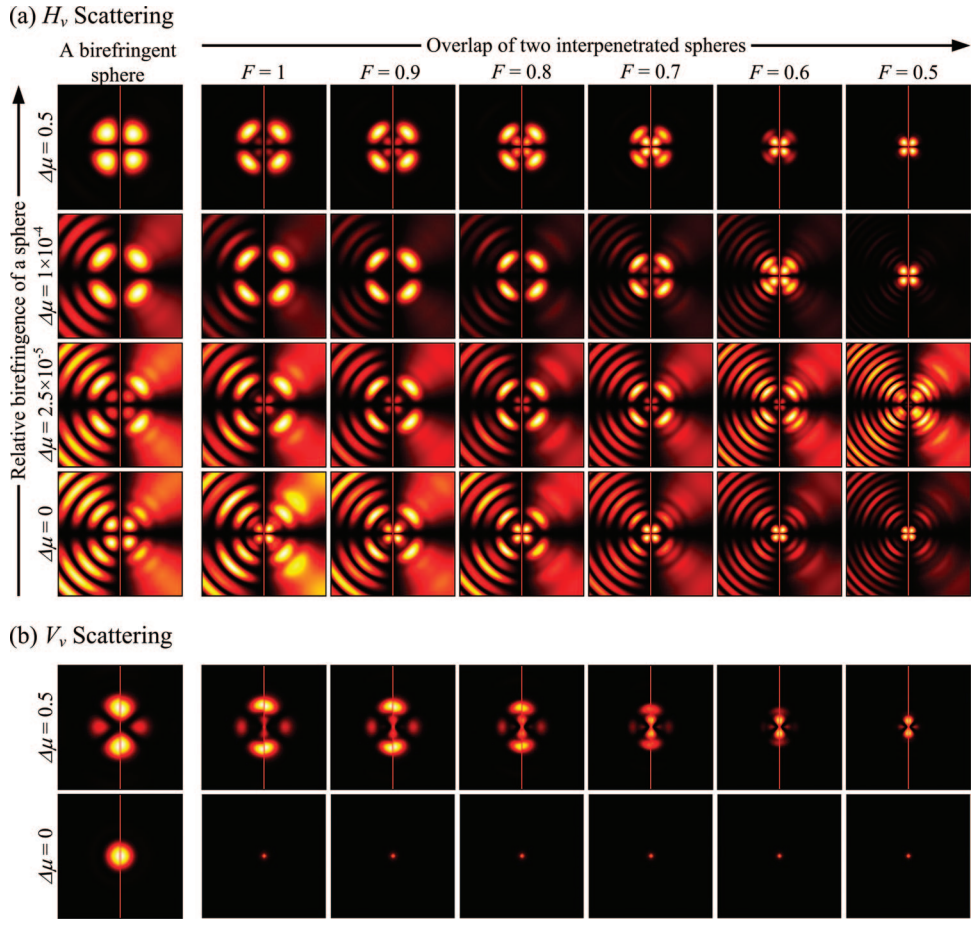

Figure 5. Calculated scattering patterns for a birefringent sphere (first column) and its aggregation (right six columns) are present as functions of the relative birefringence $\Delta\mu$ and overlapping parameter F. Other parameters are the same as shown in Figure 1. The right half of patterns show the size distribution effect on the scattering patterns for $\beta = 0.25$. (a) H_v scattering; (b) V_v scattering.

the local structure of nucleation gel evolves in the late-stage coarsening or ripening process.

A series of the calculated H_v and V_v scattering patterns for nucleation gel model are shown in parts a and b of Figure 5, respectively. The first column is for the scattering from a birefringent sphere as a function of $\Delta\mu$. The right six columns are calculated from the aggregation of birefringent spheres as functions of $\Delta\mu$ and F. In Figure 5, we also show the size distribution effect at right half of patterns. In the first, the H_v scattering to the pattern change contrast sharply with the V_v scattering. The H_v patterns highlight the feature of local-structure evolution; in contrast, the V_v patterns relate mainly to the feature of the long-range fractal structure, except the case of spherulites ($\Delta\mu = 0.5$). In fact, the H_v and V_v scattering complement each other well, for each captures a different aspect of the structural evolution of scatterers. Over the past few decades, a considerable number of studies have been made on the scattering properties of fractal aggregate; there has thus far been relatively little research on the local-structure evolution of aggregate. Here we limit the discussion to this area.

The bottom two rows in Figure 5a present excessively complicated H_v patterns. These multiple structures are formed by the aggregation of the very weakly birefringent spheres or the isotropic spheres. Up to now, there is no enough experimental evidence to prove such patterns. The reason may be explained by following two aspects. In most cases, the amorphous colloids are prepared by surface modification, so that the interparticle interaction is well approximated as the hard sphere and the coarsening or interpenetrated of two contact spheres is impossible. In contrast, for amorphous droplets, the liquidlike coalescence between two diffusing droplets (i.e., dynamic coalescence)[50,51] will govern the droplet aggregation, and the macroscopic gelation does not occur in such a case. Leaving whether such patterns exists aside, one of the thorniest problems we face is analyzing these patterns. For the very weakly birefringent sphere or the isotropic sphere, we have difficulty detected the significant difference among F values. Under this situation, the H_v scattering plays only an auxiliary role in studying the structure of amorphous aggregates. On the other hand, in the top two rows in Figure 5a, a double structure with the emergence of new first-order peak shows the main characteristics of the coarsening process of the birefringent sphere, and the steep growth of new first-order peak can be characterized by a single time-dependent length parameter a_r which offers the key to an understanding of the coarsening kinetics. On the grounds of our model, it is possible to examine whether the time evolution of the H_v scattering function can be scaled by a_r or rather whether the scaled H_v structure factor exists in late-stage coarsening. In considering this issue, we may recall the implication of the scaled structure factor and, most particularly, the specific characteristic of self-similar evolution of global structure. It is clear that the interference function is an only significant structure function in H_v scattering but can only characterize the local structure. For the reason given above, the H_v scattering is incompetent to describe the global structure evolution. More specifically, although the late-stage coarsening process can be characterized by a_r, the structure factor scaling is unsatisfactory for H_v scattering.

Conclusion

In this paper, we provide extensive discussion about the implication of the birefringence decline on studying the structure of birefringent sphere and its aggregation. In order to understand what the structural characteristic of the birefringent sphere is, we address two categories of birefringent sphere: category 1 is the crystallographic disorder, and category 2 is the aggregation of crystallitic grains. We deduce that the PVDF microgel belongs to the category 2 and can be regarded as "soft colloids". Although, scattering techniques can provide detailed information regarding the size and morphology of scatterers; however, because the dimensions of the internal structure of the birefringent sphere are much smaller than the wavelength of the light, in fact, the birefringence can only describe the average property of the scatterers. Thus, the structure model of the PVDF microgel needs to be confirmed through empirical evidence in real space. In contrast to scattering technique, the electron microscopy is a direct and available method to probe the structural morphology of the birefringent spheres. We will propose the related evidence in our next work.

The present study enhances the previous studies' findings by providing a much more detail examination of nucleation gel model and establishes methodological basis especially for depolarized scattering as applied to the recent advances in soft matter science. We present the scaled form factor to study the nucleation and growth of birefringent sphere and provide adequate structural information. In studying the heterogeneous superstructures of soft matter, the H_v and V_v scattering complement each other well, the H_v patterns highlight the feature of local-structure evolution, and the V_v patterns relate mainly to the feature of the long-range fractal structure. So far, we have seen that lacking the ability to describe the global-structure evolution, the scaling of structure factor is unsatisfactory for H_v scattering.

This study has taken an important step in the direction of studying the relationship between the methodology of depolarized SALS and soft matters with *time* and *space* complexity. In considering the subject of nucleation gel, three issues need to be resolved. Nature: what is the nonequilibration nature of gelation processes? Structure and behavior: what are the thermodynamic essences and the corresponding kinetics of the early stage nucleation? Boundary: does a metastable limit of nucleation in polymer solutions exist? These issues may be of importance in explaining the causal relationship between the complexity on mesoscopic length scale and the forming diverse morphologies of physical gels. We believe the research on nucleation gel giving us new opportunities and challenges, and we intend to probe this line of investigation in a series of experimental studies. In next work, we will focus on the topic of the scattering modeling of the nucleation gel. More specifically, the implementation of the structural formation of nucleation gel into the numerical simulation will be the next work to get the key parameters (i.e., a_0, a_r, $\Delta\mu$, μ, and β) during the structure evolution. These parameters will lead us to further research on the question of the coarsening kinetics of nucleation gel and to a better understanding of the "soft colloids" nature of PVDF microgels.

Acknowledgment. The authors thank the National Science Council of the Taiwan for financially supporting this research under Contract NSC-95-2221-E-011-090-MY3.

References and Notes

(1) Flory, P. J. *Principles of Polymer Chemistry*; Cornell University Press: London, 1975.
(2) de Gennes, P. G. *Scaling Concepts in Polymer Physics*; Cornell University Press: Ithaca, NY, 1985.
(3) Guenet, J. M. *Thermoreversible Gelation of Polymers and Biopolymers*; Academic Press: New York, 1992.
(4) te Nijenhuis, K. *Adv. Polym. Sci.* **1997**, *130*, 1.
(5) Dikshit, A. K.; Nandi, A. K. *Macromolecules* **2000**, *33*, 2616.
(6) Dasgupta, D.; Manna, S.; Garai, A.; Dawn, A.; Rochas, C.; Guenet, J. M.; Nandi, A. K. *Macromolecules* **2008**, *41*, 779.
(7) Chou, C. M.; Hong, P. D. *Macromolecules* **2004**, *37*, 5596.
(8) Chou, C. M.; Hong, P. D. *Macromolecules* **2003**, *36*, 7331.
(9) Stauffer, D; Coniglio, A.; Adam, M. *Adv. Polym. Sci.* **1982**, *44*, 105.
(10) Coniglio, A.; Stanley, H. E.; Klein, W. *Phys. Rev. Lett.* **1979**, *42*, 518.
(11) Asnaghi, D.; Giglio, M.; Bossi, A.; Righetti, P. G. *J. Chem. Phys.* **1995**, *102*, 9736.
(12) Tromp, R. H.; Rennie, A. R.; Jones, R. A. L. *Macromolecules* **1995**, *28*, 4129.
(13) Takeshita, H.; Kanaya, T.; Nishida, K.; Kaji, K. *Macromolecules* **1999**, *32*, 7815.
(14) Hong, P. D.; Chou, C. M. *Macromolecules* **2000**, *33*, 9673.
(15) Lorén, N.; Altskär, A.; Hermansson, A. M. *Macromolecules* **2001**, *34*, 8117.
(16) Trappe, V.; Prasad, V.; Cipelletti, L.; Segre, P. N.; Weitz, D. A. *Nature (London)* **2001**, *411*, 772.
(17) Liu, A. J.; Nagel, S. R. *Nature (London)* **1998**, *396*, 21.
(18) Stein, R. S.; Rhodes, M. B. *J. Appl. Phys.* **1960**, *31*, 1873.
(19) Stein, R. S.; Wilson, P. R. *J. Appl. Phys.* **1962**, *33*, 1914.
(20) Rhodes, M. B.; Stein, R. S. *J. Polym. Sci., Part A2* **1969**, *7*, 1538.
(21) Koberstein, J.; Russell, T. P.; Stein, R. S. *J. Polym. Sci., Part B: Polym. Phys.* **1979**, *17*, 1719.
(22) Yoon, D. Y.; Stein, R. S. *J. Polym. Sci., Part B: Polym. Phys.* **1974**, *12*, 763.
(23) Meeten, G. H.; Navard, P. *J. Polym. Sci., Part B: Polym. Phys.* **1984**, *22*, 2159.
(24) Desborder, M.; Meeten, G. H.; Navard, P. *J. Polym. Sci., Part B: Polym. Phys* **1989**, *27*, 2037.
(25) Champion, J. V.; Killey, A.; Meeten, G. H. *J. Polym. Sci., Part B: Polym. Phys.* **1985**, *23*, 1467.
(26) Meeten, G. H.; Navard, P. *J. Polym. Sci., Part B: Polym. Phys.* **1989**, *27*, 2023.
(27) Van de Hulst, H. C. *Light Scattering by Small Particles*; John Wiley & Sons: New York, 1957.
(28) Cipelletti, L.; Ramos, L. *Curr. Opin. Colloid Interface Sci.* **2002**, *7*, 228.
(29) Trappe, V.; Sandkühler, P. *Curr. Opin. Colloid Interface Sci.* **2004**, *8*, 494.
(30) Scheffold, F.; Cerbino, R. *Curr. Opin. Colloid Interface Sci.* **2007**, *12*, 50.
(31) Motegi, M.; Oda, T.; Moritani, M.; Kawai, H. *Polym. J.* **1970**, *1*, 209.
(32) Gránásy, L.; Pusztai, T.; Tegze, G.; Warren, J. A.; Douglas, T. F. *Phys. Rev. E* **2005**, *72*, 011605.
(33) Binder, K.; Stauffer, D. *Phys. Rev. Lett.* **1974**, *33*, 1006.
(34) Binder, K. *Phys. Rev. B* **1977**, *15*, 4425.
(35) Roe, R. J. *Methods of X-ray and Neutron Scattering in Polymer Science*; Oxford Univserity Press: New York, 2000.
(36) Takenaka, M.; Hashimoto, T. *J. Chem. Phys.* **1992**, *96*, 6177.
(37) Park, I. H.; Yoon, J. E.; Kim, Y. C.; Yun, L.; Lee, S. C. *Macromolecules* **2004**, *37*, 6170.
(38) Filobelo, L. F.; Galkin, O.; Vekilov, P. G. *J. Chem. Phys.* **2005**, *123*, 014904.
(39) Vekilov, P. G. *Cryst. Growth Des.* **2004**, *4*, 671.
(40) Moritani, M.; Inoue, T.; Motegi, M.; Kawai, H. *Macromolecules* **1970**, *3*, 433.
(41) Cho, H.; Song, Y.; Kim, S. Y. *Polymer* **1993**, *34*, 1024.
(42) Kataoka, H.; Saito, Y.; SaKai, T.; Quartarone, E.; Mustarelli, P. *J. Phys. Chem. B* **2000**, *104*, 11460.
(43) Jana, T.; Rahman, M.; Nandi, A. K. *Colloid Polym. Sci.* **2004**, *282*, 555.
(44) Cipelletti, L.; Manley, S.; Ball, R. C.; Weitz, D. A. *Phys. Rev. Lett.* **2000**, *84*, 2275.
(45) Segrè, P. N.; Prasad, V.; Schofield, A. B.; Weitz, D. A. *Phys. Rev. Lett.* **2001**, *86*, 6042.
(46) Lifahitz, I. M.; Slyozov, V. V. *J. Phys. Chem. Solids* **1961**, *19*, 35.
(47) Wagner, C. *Z. Electrochem.* **1961**, *65*, 518.
(48) Stanley, H. E.; Ostrowski, N. *On Growth and Form: Fractal and Non-Fractal Patterns in Physics*; Nijhoff: Dordrecht, 1986.000
(49) Dubois, J.; Fyen, W.; Rusu, D.; Peuvrel-Disdier, E.; Navard, P. *J. Polym. Sci., Part B: Polym. Phys.* **1998**, *36*, 2005.
(50) Nikolayve, V. S.; Beysens, D.; Guenoun, P. *Phys. Rev. Lett.* **1996**, *76*, 3144.
(51) Rosenfeld, G.; Morgenstern, K.; Esser, M.; Comsa, G. *Appl. Phys. A* **1999**, *69*, 489.

MA702765U